

**A Phase-change Gel based pressure sensor with tunable sensitivity for artificial  
tactile feedback system**

Houchao Jing,<sup>ab</sup> Lin Xu,<sup>ab</sup> Xuanqi Wang,<sup>c</sup> Yaqing Liu,<sup>\*ab</sup> and Jingcheng Hao<sup>a</sup>

<sup>a</sup>Key Laboratory of Colloid and Interface Chemistry of the Ministry of Education, School of Chemistry and Chemical Engineering, Shandong University, Jinan, Shandong, 250100, China. E-mail: [liuyaqing@sdu.edu.cn](mailto:liuyaqing@sdu.edu.cn)

<sup>b</sup>Suzhou Research Institute, Shandong University, Suzhou, Jiangsu, 215123, China.

<sup>c</sup>School of Software, Shandong University, Jinan, Shandong, 250101, China.

Supplementary Video S1. Adaptive grasping performances of an artificial tactile feedback system.

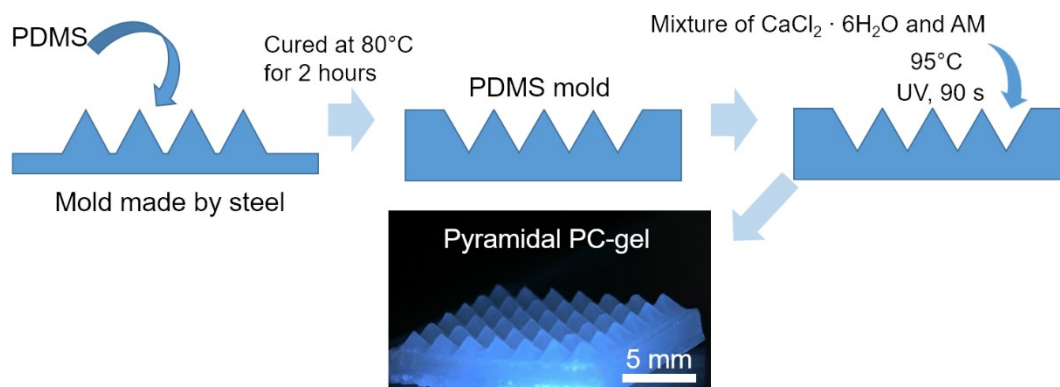


**Figure S1.** Fabrication process of a pyramidal PC-gel film.

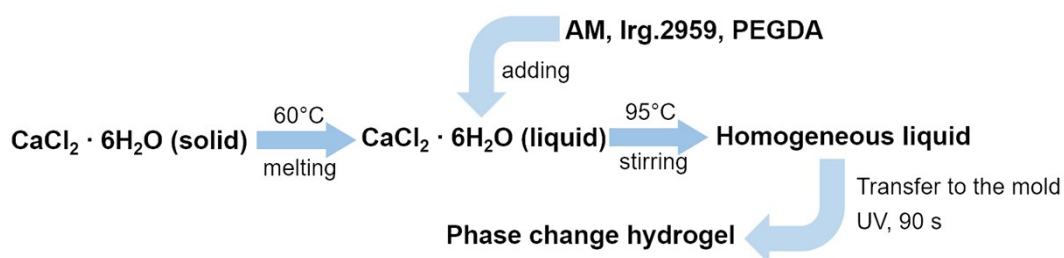


**Figure S2.** Synthesis of phase-change gel with acrylamide and calcium chloride hexahydrate.

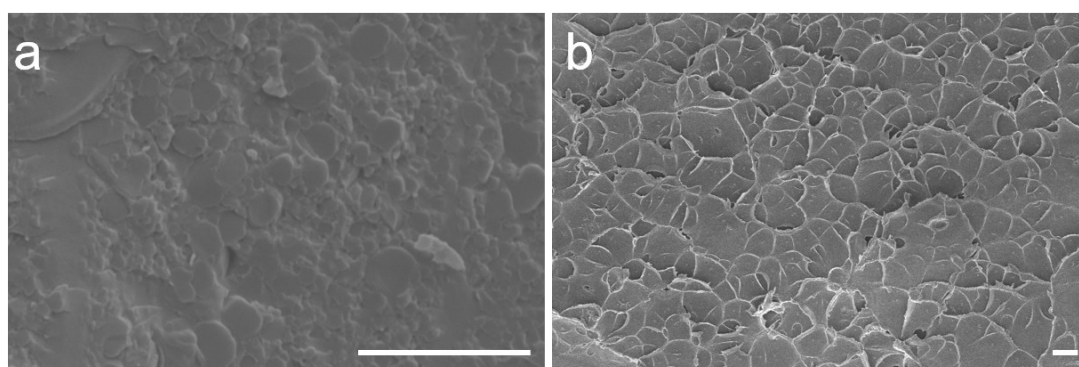


**Figure S3.** (a) Cryo-SEM images of a PC-gel in rigid state, (b) SEM image of a PC-gel in soft state processed by solvent replacement method. (Scale bar: 10 $\mu$ m)

In order to maintain the integrity of the hydrogel's network, freeze-drying is a common

processing method to prepare samples for SEM test. However, such method cannot be used for PC-gel in soft state directly, due to the PC-gel switched to rigid state during freeze-drying. To remove water inside PC-gel in soft state, we used the solvent replacement method. As the gel fibers cannot form a self-supporting structure due to the loss of water, the SEM image presented a wrinkled gel film.

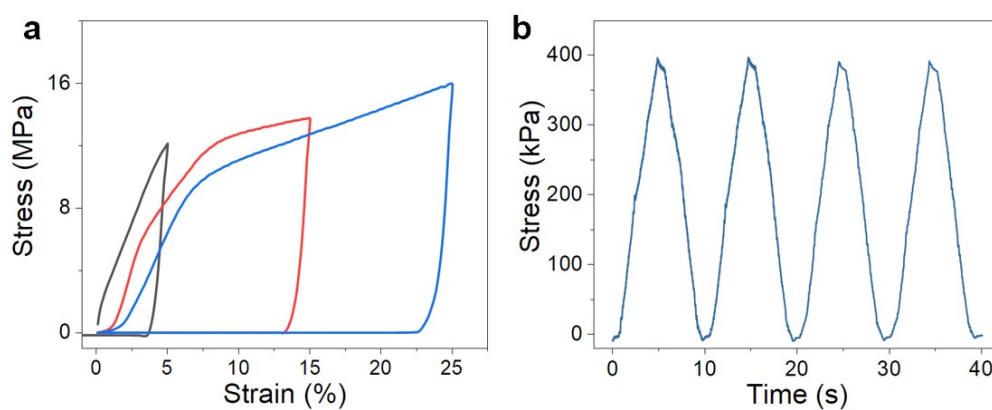


**Figure S4.** (a) Consecutive cyclic tensile loading-unloading curves for the PC-gel in rigid state under different strains. (b) Stress variation with time upon dynamic 1% strain (the crosshead speed: 1 mm/min).

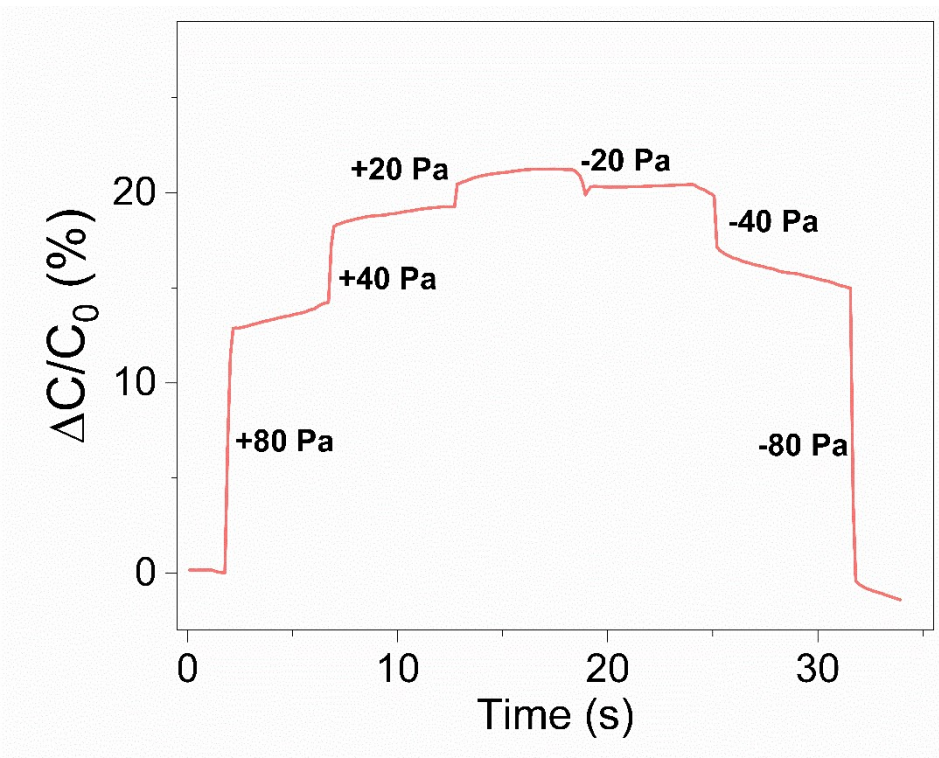


**Figure S5.** Real-time reading of the relative capacitance change by a PC-gel-based pressure sensor in **Mode I** under different loadings.

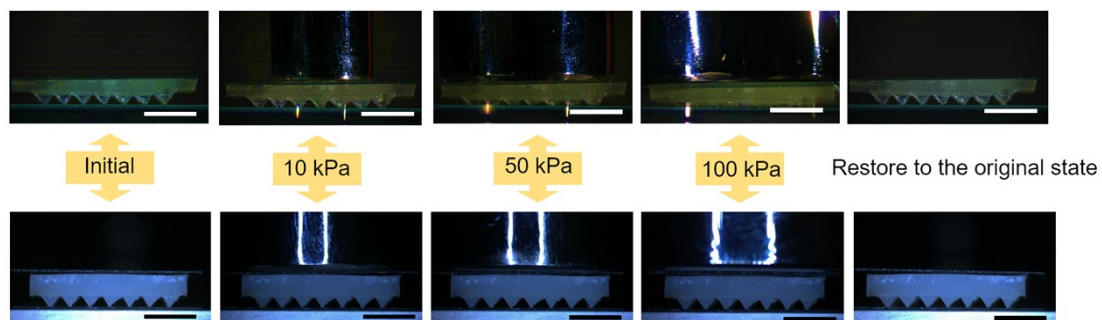


**Figure S6.** The deformation of the pyramidal PC-gel films in soft state (up) and rigid state (down) under different stresses. (Scale bar: 5 mm)

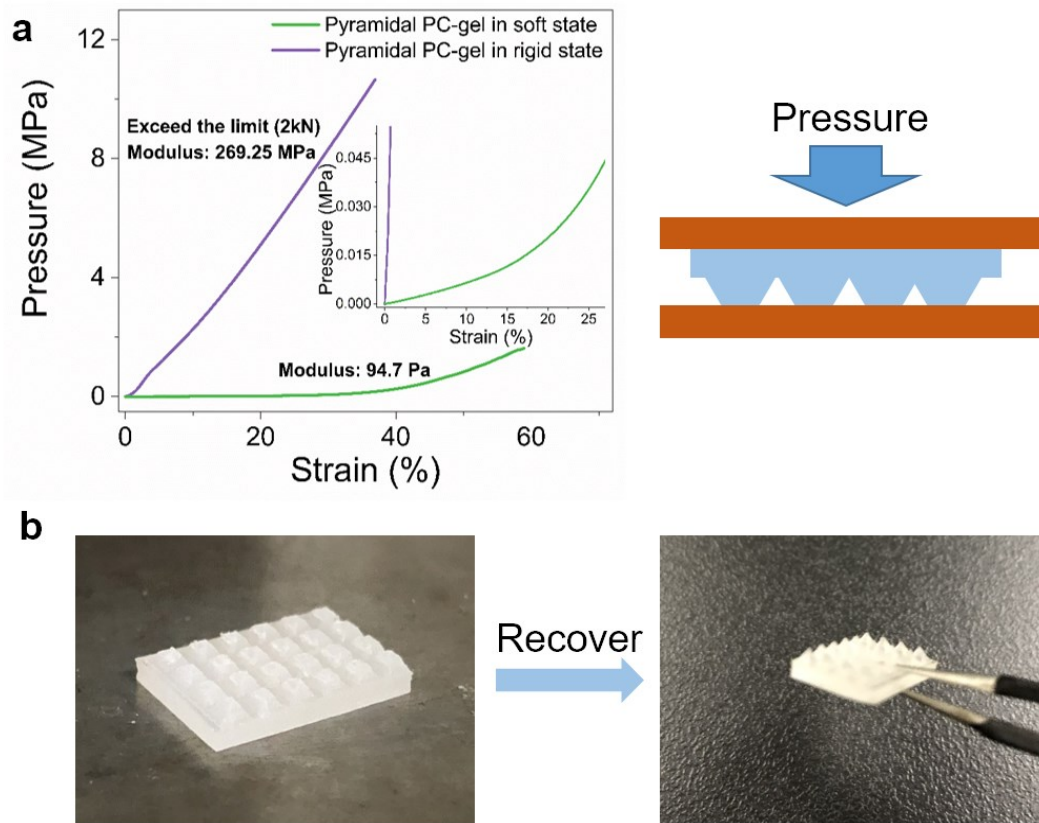


**Figure S7.** (a). The stress-strain curve of pyramidal PC-gel films in soft or rigid states, and the schematic diagram of compression test. (b) After been pressed at 10 MPa, the pyramidal structure on the surface of PC-gel was flattened, which can totally recover after phase changing at high temperature.

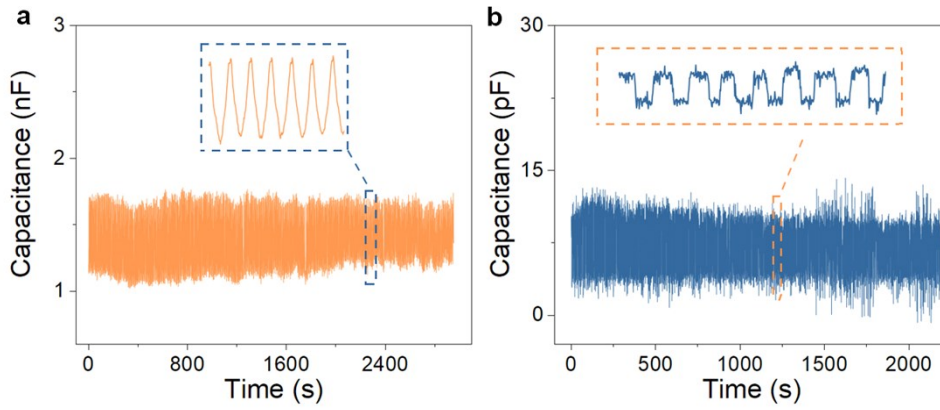


**Figure S8.** The stability of the pressure sensor in two operating modes. (a) Capacitance reading of a PC-gel-based pressure sensor in **Mode II** under repeated loading of 5.5 kPa. (b) A PC-gel-based pressure sensor in **Mode II** subjected to the manual loading of 100 kPa for 500 cycles.

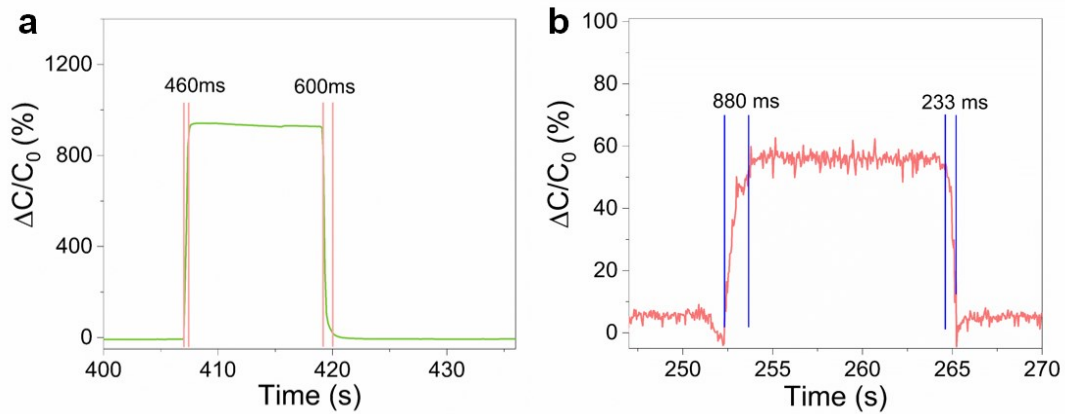


**Figure S9.** Response time of PC-gel-based pressure sensors in **Mode I** (a) and **Mode II** (b) under the loading pressure of 0.7 kPa and 100 kPa, respectively.

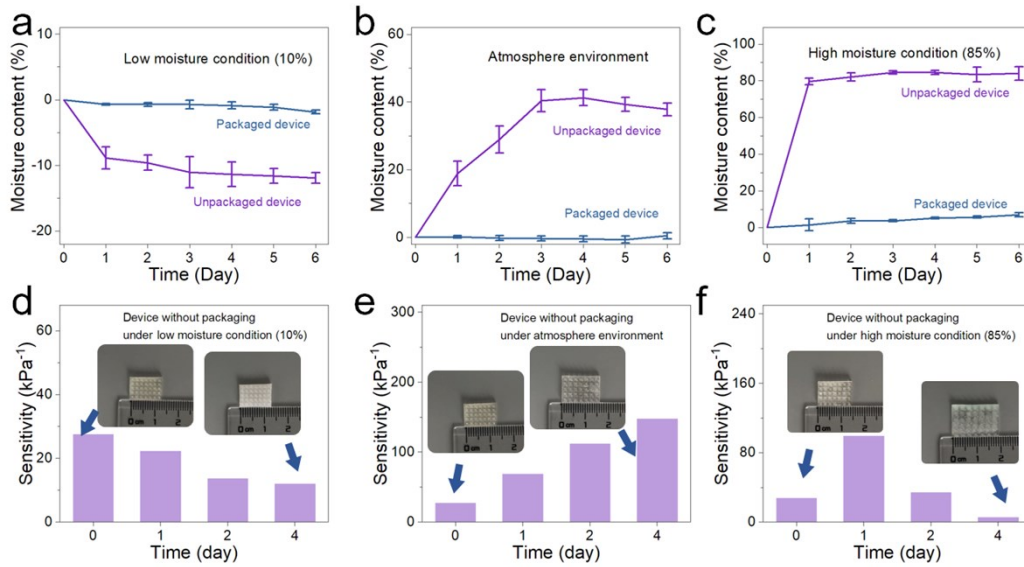


**Figure S10.** The moisture content and sensitivity of packaged and unpackaged devices in atmosphere environment (a, d), high moisture condition (b, e). For sensors stored in atmosphere and high moisture conditions, as moisture is absorbed, sensitivity is increased due to electric double layer. And the subsequent drop in sensitivity under the high moisture condition is due to structural collapse. The moisture content (c) and sensitivity (f) of packaged and unpackaged devices in low moisture condition. For sensors stored in low moisture condition, the loss of water and the precipitation of inorganic salts will reduce the compression properties of the sensor. Therefore, the sensitivity decrease with storing time.

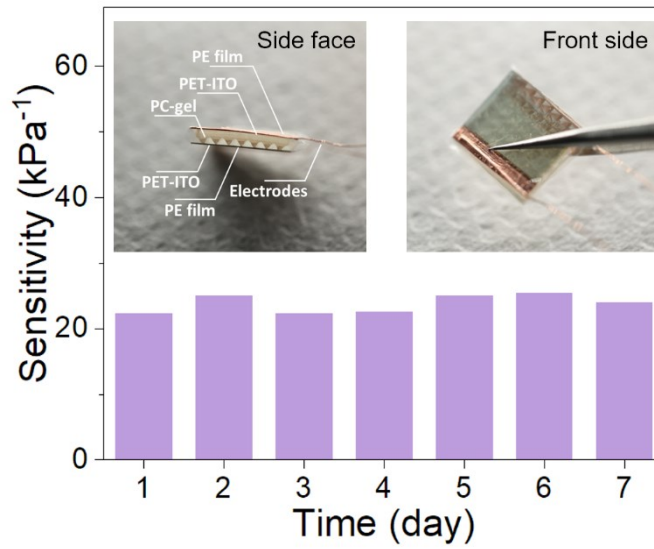


**Figure S11.** The sensitivity of a packaged sensor stored at ambient condition for one week.

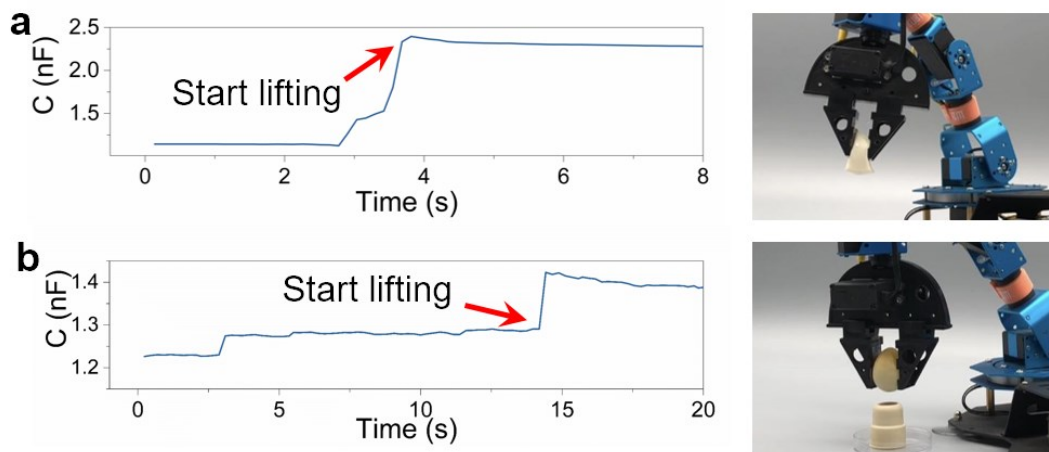


**Figure S12.** Capacitance response and the photographs of grasping a piece of tofu and a naked egg by the robotic gripper with PC-gel-based pressure sensor operating in **Mode I**.

Table S1. The summary and comparison of the capacitance-type pressure sensors based on different materials.

Active materials	Sensitivity	Working range	characteristics	Reference
H <sub>3</sub> PO <sub>4</sub> /PVA hydrogel	> 220 kPa <sup>-1</sup>	0.08 Pa to 360 kPa	High sensitivity with ultrabroad - range	1
polyaniline spheres /poly(vinyl alcohol) /phytic acid hydrogel	3.6 kPa <sup>-1</sup>	< 0.1 kPa	Pressure /strain sensors	2
Graphene / PDMS /nylon	0.33 kPa <sup>-1</sup>	3.3 Pa to 5 kPa		3
Sodium alginate /acrylic acid hydrogel	0.17 kPa <sup>-1</sup>	< 1 kPa	Highly Sensitive Pressure Sensing	4
Pectin /poly(acrylic acid) /metal ions hydrogel	0.655 kPa <sup>-1</sup> under 0 - 15 kPa and 0.24 kPa <sup>-1</sup> under 15 -25 kPa	< 25 kPa	Stretchable and self-healable capacitance pressure	5
P(VDF-HFP) /ionic liquid	41 kPa <sup>-1</sup> under < 400 Pa	< 50 kPa	Broad-Range Pressures with High Sensitivity	6
P(VDF-HFP) /ionic liquid	54.31 kPa <sup>-1</sup> under < 0.5 kPa	0.1 Pa to 115 kPa	High sensitivity and broad-range pressure	7
Carbon nanotube /poly(dimethylsiloxane) /ion-gel	9.55 kPa <sup>-1</sup>		Detecting Static and Dynamic Pressure	8
Our work	21 kPa <sup>-1</sup> in <b>Mode I</b> and 0.42 kPa <sup>-1</sup> in <b>Mode II</b>	2 Pa to 350 kPa	Tunable sensitivity and working range	

The pressure sensor presents a high sensitivity up to 21 kPa<sup>-1</sup> and a broad sensing range up to 350 kPa, which exceed many capacitance-type pressure sensors based on different materials.

## Reference:

1. N. N. Bai, L. Wang, Q. Wang, J. Deng, Y. Wang, P. Lu, J. Huang, G. Li, Y. Zhang, J. L. Yang, K. W. Xie, X. H. Zhao and C. F. Guo, *Nat. Commun.*, 2020, **11**, 209.
2. H. Zhou, Z. Wang, W. Zhao, X. Tong, X. Jin, X. Zhang, Y. Yu, H. Liu, Y. Ma, S. Li and W. Chen, *Chem. Eng. J.*, 2021, **403**, 126307.
3. Z. He, W. Chen, B. Liang, C. Liu, L. Yang, D. Lu, Z. Mo, H. Zhu, Z. Tang and X. Gui, *ACS Appl. Mater. Interfaces*, 2018, **10**, 12816-12823.
4. Z. Lei, Q. Wang, S. Sun, W. Zhu and P. Wu, *Adv. Mater.* , 2017, **29**, 1700321.
5. S. Dai, S. Wang, H. Yan, J. Xu, H. Hu, J. Ding and N. Yuan, *Mater. Res. Express* 2019, **6**, 0850b0859.
6. S. H. Cho, S. W. Lee, S. Yu, H. Kim, S. Chang, D. Kang, I. Hwang, H. S. Kang, B. Jeong, E. H. Kim, S. M. Cho, K. L. Kim, H. Lee, W. Shim and C. Park, *ACS Appl. Mater. Interfaces*, 2017, **9**, 10128-10135.
7. Z. Qiu, Y. Wan, W. Zhou, J. Yang, J. Yang, J. Huang, J. Zhang, Q. Liu, S. Huang, N. Bai, Z. Wu, W. Hong, H. Wang and C. F. Guo, *Adv. Funct. Mater.* , 2018, **28**, 1802343.
8. S. G. Yoon, B. J. Park and S. T. Chang, *ACS Appl. Mater. Interfaces*, 2017, **9**, 36206-36219.